Single Crystalline Submicrotubes from Small Organic Molecules

Yong Sheng Zhao,[†,‡] Wensheng Yang,[†,§] Debao Xiao,[†] Xiaohai Sheng,[†] Xia Yang,[∥] Zhigang Shuai,[∥] Yi Luo,[⊥] and Jiannian Yao*[,†]

Key Laboratory of Photochemistry, Center for Molecular Science, Institute of Chemistry, Chinese Academy of Sciences, Beijing 100080, China, College of Chemistry, Jilin University, Changchun 130023, China, Key Laboratory of Organic Solid, Center for Molecular Science, Institute of Chemistry, Chinese Academy of Sciences, Beijing 100080, China, Theoretical Chemistry, Royal Institute of Technology, SCFAB, S-106 91 Stockholm, Sweden, and Graduate School, Chinese Academy of Sciences, Beijing 100039, China

Received August 29, 2005. Revised Manuscript Received October 20, 2005

The single crystalline submicrotubes of a small organic functional molecule, 2,4,5-triphenylimidazole (TPI), were successfully prepared with a facile method. A series of characterizations indicated that the tubes were obtained from the rolling followed by seaming of a preorganized two-dimensional sheet-like structure, whose formation was due to the efficient cooperation of several molecular recognition elements. The length and diameter of the TPI tubes can be readily controlled by adjusting the experimental conditions. The as-prepared submicrotubes have intensive luminescence and size-dependent optical properties, which allows them to find potential applications in novel optical and optoelectronic devices together with their single crystalline structure and good stability. The strategy described here should give a useful enlightenment for the design and fabrication of tubular structures from small organic molecules.

Introduction

During the past decades, one-dimensional nano- and submicrostructures, especially tubular ones, have attracted extensive investigation due to their unique optical and electronic properties[1] and their potential applications in various fields such as optoelectronics, catalysis, energy storage, and so on.[2−5] However, most of the present works were focused on inorganics and macromolecules[6−8] whereas less attention has been paid to tubes from low-molecular-weight organic compounds although it is well-known that the electronic and optical properties of organic low-dimensional materials are fundamentally different from those of inorganic ones,[9−12] because the intermolecular interactions are of the noncovalent types, such as hydrogen bond (H-bond), $\pi-\pi$ interaction, van der Waals contact, and charge transfer (CT) interaction. Owing to their diversity, tailorability, and multifunctionality, it is of great significance to extend the relative researches to small organic molecules.

So far, most of organic nano- and submicrotubes are fabricated from the self-stacking of disk-like molecules[7,13,14] and the self-assembly of multifunctional molecules such as dendrimers[15] and amphiphiles.[16] Template method[17,18] has been applied to prepare organic nanotubes but most of the products have amorphous structures. Extensive studies on inorganic nanotubes[19−21] suggest that a more readily way to prepare tubules is through the rolling of lamellar structures. It has been proposed that there also exists the possibility to acquire organic nanotubes by the rolling mechanism.[22,23] There have been some reports on the construction of two-dimensional (2D) lamellar supramolecular structures via molecular recognition elements such as hydrogen bond (H-bond), $\pi-\pi$ interaction, van der Waals contact, etc. from organic molecules.[24,25] However, to the best of our knowl-

* Correspondening author. E-mail: jnyao@iccas.ac.cn.
[†] Key Laboratory of Photochemistry, Institute of Chemistry, Chinese Academy of Sciences.
[‡] Graduate School, Chinese Academy of Sciences.
[§] Jilin University.
[∥] Key Laboratory of Organic Solids, Institite of Chemistry, Chinese Academy of Sciences.
[⊥] Royal Institute of Technology.

(1) Xia, Y.; Yang, P.; Sun, Y.; Wu, Y., Mayers, B.; Gates, B.; Yin, Y.; Kim, F.; Yan, H. *Adv. Mater.* **2003**, *15*, 353.
(2) Hu, J.; Ouyang. M.; Yang, P.; Lieber, C. M. *Nature* **1999**, *399*, 48.
(3) Che, G.; Lakshmi, B. B.; Fisher, E. R.; Martin, C. R. *Nature* **1998**, *393*, 346.
(4) Collins, P. G.; Zettl, A.; Bando, H.; Thess, A.; Smalley, R. E. *Science* **1997**, *278*, 100.
(5) Star, A.; Lu, Y.; Bradley, K.; Gruner, G. *Nano Lett.* **2004**, *4*, 1587.
(6) Parthasarathy, R. V.; Martin, C. R. *Nature* **1994**, *369*, 298.
(7) Ghadiri, M. R.; Granja, J. R.; Milligan, R. A., McRee, D. E., Khazanovich, N. *Nature* **1993**, *366*, 324.
(8) Yan, D.; Zhou, Y.; Hou, J. *Science* **2004**, *303*, 65.
(9) Fu, H. B.; Yao, J. N. *J. Am. Chem. Soc.* **2001**, *123*, 1434.
(10) Fu, H. B.; Loo, B. H.; Xiao, D. B.; Xie, R. M.; Ji, X. H.; Yao, J. N.; Zhang, B. W.; Zhang, L. Q. *Angew. Chem., Int. Ed.* **2002**, *41*, 962.
(11) Xiao, D. B.; Xi, L.; Yang, W. S.; Fu, H. B.; Shuai, Z. G.; Fang, Y.; Yao, J. N.; *J. Am. Chem. Soc.* **2003**, *125*, 6740.
(12) Tian, Z. Y.; Chen, Y.; Yang, W. S.; Yao, J. N.; Zhu, L. Y.; Shuai, Z. G. *Angew. Chem. Int. Ed.* **2004**, *43*, 4060.
(13) Bong, D. T.; Clark, T. D.; Granja, J. R.; Ghadiri, M. R. *Angew. Chem., Int. Ed.* **2001**, *40*, 988.
(14) Hong, B. H.; Lee, J. Y.; Lee, C. W.; Kim, J. C.; Bae, S. C.; Kim, K. S. *J. Am. Chem. Soc.* **2001**, *123*, 10748.
(15) Yamaguchi, T.; Ishii, N.; Tashiro, K.; Aida, T. *J. Am. Chem. Soc.* **2003**, *125*, 13934.
(16) John, G.; Masuda, M.; Okada, Y.; Yase, K.; Shimizu, T. *Adv. Mater.* **2001**, *13*, 715.
(17) Martin, C. R. *Science* **1994**, *266*, 1961.
(18) Zhao, L. Y.; Yang, W. S.; Ma, Y.; Yao, J. N.; Li, Y. L.; Liu, H. B. *Chem. Commun.* **2003**, 2442.
(19) Iijima, S. *Nature* **1991**, *354*, 56.
(20) Schaak, R. E.; Mallouk, T. E. *Chem. Mater.* **2000**, *12*, 3427.
(21) Li, Y. D.; Li, X. L.; He, R. R.; Zhu, J.; Deng, Z. X. *J. Am. Chem. Soc.* **2002**, *124*, 1411.
(22) Hartgerink, J. D.; Clark. T. D.; Ghadiri, M. R. *Chem. Eur. J.* **1998**, *4*, 1367.
(23) Langley, P. J.; Hulliger, J. *Chem. Soc. Rev.* **1999**, *28*, 279.

10.1021/cm051949t CCC: $30.25
Published on Web 11/15/2005

Scheme 1. Chemical Structure (a) and Optimized Geometry (b) of Single 2,4,5-Triphenylimidazole (TPI) Molecule

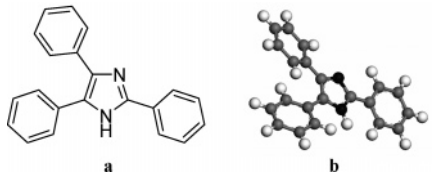

edge, the construction of organic tubes via the rolling of lamellar structures has hardly been described in practice.

Herein, for the first time, we describe the fabrication of a single crystalline submicrotube from a small organic functional molecule, 2,4,5-triphenylimidazole (TPI) (Scheme 1), via the rolling and seaming of a 2D lamellar structure, directed by the cooperation of several noncovalent interactions. The length and diameter of the as-fabricated TPI tubes can be readily controlled by adjusting the experimental conditions such as temperature and sonication time. The submicrotubes have intensive luminescence, size-dependent optical properties, and good stability, which allow them to find potential applications in novel optical and optoelectronic devices. The strategy described here should give a useful enlightenment for the design and fabrication of tubular structures from small organic molecules.

Experimental Section

Materials. The model compound used in our work, 2,4,5-triphenylimidazole (Scheme 1), was purchased from Sigma-Aldrich and used without further treatment. Ultrapure water with a resistivity of 18.2 MΩ·cm, which acts as the poor solvent, was produced using a Milli-Q apparatus (Millipore, America) and was filtered using inorganic membrane with a pore size of 0.02 μm (Whatman International Ltd) just before use.

Procedure. The TPI submicrotubes were prepared through a facile reprecipitation method. In a typical preparation, 400 μL of TPI stock solution in good solvent such as ethanol or acetone (10^{-3} M) was injected rapidly (<2 s) into 10 mL of ultrapure water of different temperatures, which acts as the poor solvent, followed by different times of sonication. The changing of the solvent surroundings can induce the nucleation and growth of TPI nanotubes. The wavelength of the ultrasound is about 4 μm. The TPI solution was filtered by using an inorganic membrane filter with 0.02 μm pore size (Whatman International Ltd.) before the injection.

The morphologies and sizes of the as-prepared TPI submicrotubes were examined by scanning electron microscopy (SEM, Hitachi S-4300) and transmission electron microscopy (TEM, JEOL JEM-2010). For preparation of the SEM samples, a drop of the as-prepared dispersion was deposited onto a freshly cleaned wafer. To enhance the conductivity of the sample, a layer of platinum was sputtered at a current of 5 mA and a pressure of 3 mmHg. The TEM samples were made by placing a drop of the as-prepared dispersion of the tubes gently onto the TEM grid.

X-ray diffraction patterns of the TPI powder and TPI tube samples were carried out on a Japan Rigaku D/max-2500 rotation anode X-ray diffractometer equipped with graphite monochromatized Cu Kα radiation (λ = 1.5418 Å) after being filtered onto porous alumina membranes (Whatman Ltd., 0.02 μm).

The temperature-dependent ^{1}H NMR spectra for TPI submicrotubes were carried out on a Bruke 600 Hz NMR instrument. Deuterated DMSO and deuterated water were used as the good and poor solvents, respectively. The X-ray photoelectron spectra (XPS) were recorded on a USW HA150 photoelectron spectrometer at BSRF using an Al Kα (1486.6 eV) monochromatic X-ray source.

The UV−visible absorption spectra of the TPI submicrotubes dispersed in water were measured using a Shimadzu UV-1601 PC double-beam spectrophotometer. The fluorescence spectra and fluorescence quantum yield were measured using a Hitachi F-4500 fluorospectrometer. FESEM measurements indicated that, during the above optical characterization, the average sizes and the size distributions of the tubes did not experience obvious changes.

The molecular geometries of TPI molecule and its supramolecular structures were drawn, and the minimum energy configuration was optimized using the semiempirical AM1 (Austin Model 1) method[26] as implemented in AMPAC program package.[27] In the actual nanotubes, a number of different intermolecular separations and relative orientations of the molecules are likely to be present. To investigate the dependence of the results on the choice of intermolecular geometric parameters, we have repeated the same calculations by varying the intermolecular position and different packing models.

Results and Discussion

The typical SEM images, as shown in Figure 1A and B, suggest that the as-fabricated TPI submicrotubes have comparatively high monodispersity and that each tube has rather smooth surface and uniform diameter all through the entire length. The TEM pictures (Figure 1C) show that the tubes have open-ended structures. The selected area electron diffraction (SAED) pattern (Figure 1D) indicates that the tubes have single crystalline structure and that the tube axis is the *c* axis of TPI crystal. This conclusion is further supported by the XRD patterns (Figure 2), which indicate the preferential orientation of (001) lattice plane in TPI tubes.

SEM images (Figure 3) illustrate the evolution of the submicrotubes with the aging time. It is likely that the TPI molecules tend to form a sheet-like structure at the beginning (Figure 3A) and the lamellar structures are partially rolled at the two sides after 5 min ripening (Figure 3B). Then the curled sheets tend to be seamed at the edges, and finally the tubes are observed after ripened for 30 min (Figure 3C). This suggests that the curling and seaming of a preorganized sheet-like structure is responsible for the formation of the tubes.

It is known that different dominant intermolecular interactions are responsible for the formation of organic nano- and submicrostructures with different shapes.[12] The interactions that play decisive roles in the formation of organic low-dimensional structures are those noncovalent forces such as H-bond, $\pi-\pi$ interaction, intermolecular charge transfer (Inter-CT), van der Waals contact, etc. Among those noncovalent forces, H-bond is expected to be the most efficient one in determining the morphology of the finally obtained structures.[28] The temperature-dependent ^{1}H NMR spectra for TPI nanotubes shown in Figure 4 indicate that the chemical

(24) Kloster, R. A.; Carducci, M. D.; Mash, E. A. *Org. Lett.* **2003**, *5*, 3683.
(25) Holder, S. J.; Elemans, J. A. A. W.; Donners, J. J. J. M.; Boerakker, M. J.; de Gelder, R.; Barbera, J.; Rowan, A. E.; Nolte, R. J. M. *J. Org. Chem.* **2001**, *66*, 391.
(26) Dewar, M. J. S.; Zoebisch, E. G.; Healy, E. F.; Stewart, J. J. P. *J. Am. Chem. Soc.* **1985**, *107*, 3898−3902.
(27) AMPAC. Semichem: 7204 Mullen, Shawnee, KS, 2002.
(28) Prins, L. J.; Reinhoudt, D. N.; Timmerman, P. *Angew. Chem., Int. Ed.* **2001**, *40*, 2382.

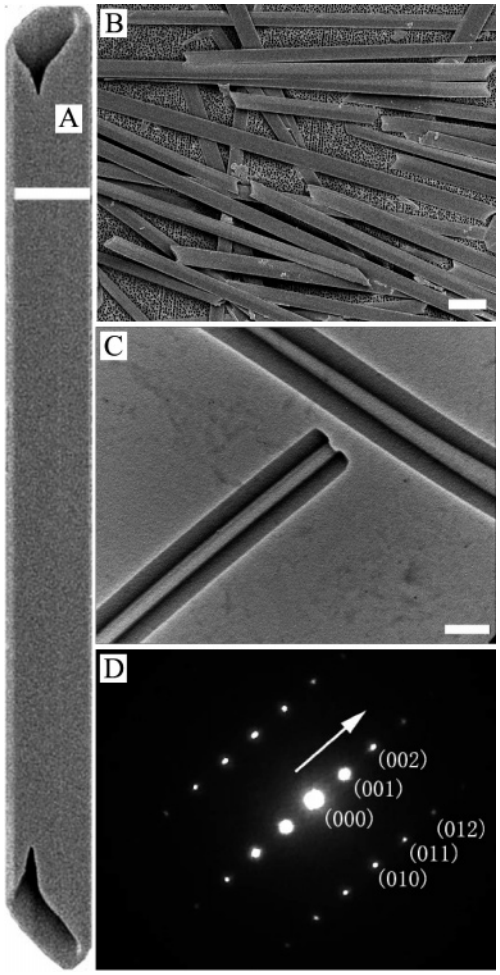

Figure 1. Electron microscopy images and SAED pattern of the as-prepared TPI submicrotubes. (A) Typical SEM image of a single tube, scale bar is 200 nm. (B) SEM image of the tubes, scale bar is 500 nm. (C) TEM image of the tubes, scale bar is 200 nm. (D) SAED pattern of the tubes along [100] zone axis with the main diffraction spot indexed. The arrow indicates the direction of the tube axis. All the samples were prepared at 60 °C with 20 s sonication treatment.

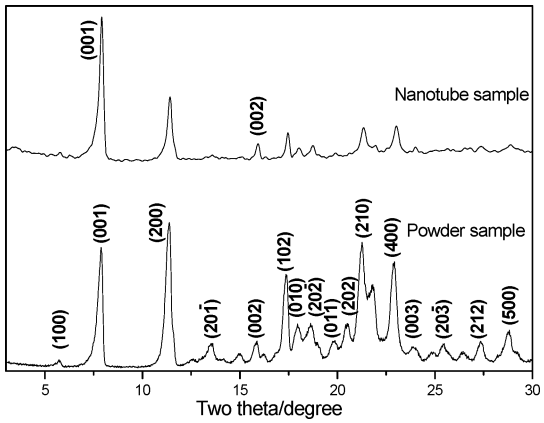

Figure 2. XRD experimental results of the TPI powder sample and the TPI tube sample.

shift of the active H atom move to high field with the increase of temperature and the absolute value of the average temperature coefficient is 3.75 ppb/K, which can prove the existence of H-bonds between the N−H group of one TPI molecule and the pyridine-type N atom of the neighboring one in the tubes.[29] The measurements of N1s XPS also testified the formation of large quantity of N−H...N H-bonds[30] (see Supporting Information). It is expected that the H-bonds between the TPI molecules will result in the formation of supramolecular chains, which is supposed to be the prerequisite to the formation of TPI submicrotubes.

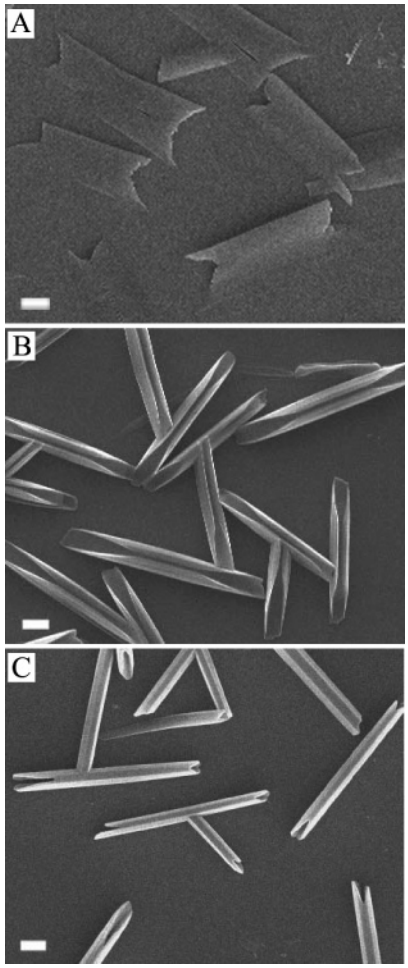

Figure 3. SEM images of TPI submicrotubes ripened for different time prepared at 25 °C. (A) Without ripening. (B) Ripened for 5 min. (C) Ripened for 30 min. All the scale bars correspond to 250 nm.

The noncovalent interactions between TPI molecules in the submicrotubes were further investigated by the UV−visible spectra (see Supporting Information). TPI monomers in ethanol exhibit two resolved absorption bands at 302 nm (4.10 eV) and 227 nm (5.46 eV) attributed to the $S_0 \rightarrow S_1$ transition (see Supporting Information) and the transition of phenyl rings, respectively. For the tubes with a diameter of 250 nm, a new band at about 340 nm (3.65 eV) emerges. The new band is in well consistent with the theoretically calculated result of the Inter-CT transition between the corresponding TPI molecules in the neighboring H-bonded chains (see Supporting Information), attributed to the geometry of maximum face to face overlap of the aromatic rings. The maximum overlap is promoted by the solvophobic effects in poor solvent systems[31] and can bring strong $\pi-\pi$ interactions between the supramolecular chains, which result in the formation of 2D sheet-like structures. Moreover, the

(29) Bekiroglu, S.; Kenne, L.; Sandstrom, C. *J. Org. Chem.* **2003**, *68*, 1671.
(30) O'Shea, J. N.; Schnadt, J.; Bruhwiler, P. A.; Hillesheimer, H.; Martensson, N.; Patthey, L.; Krempasky, J.; Wang, C.; Luo, Y.; Agren, H. *J. Phys. Chem. B* **2001**, *105*, 1917.
(31) Hunter, C. A.; Sanders, J. K. M. *J. Am. Chem. Soc.* **1990**, *112*, 5525.

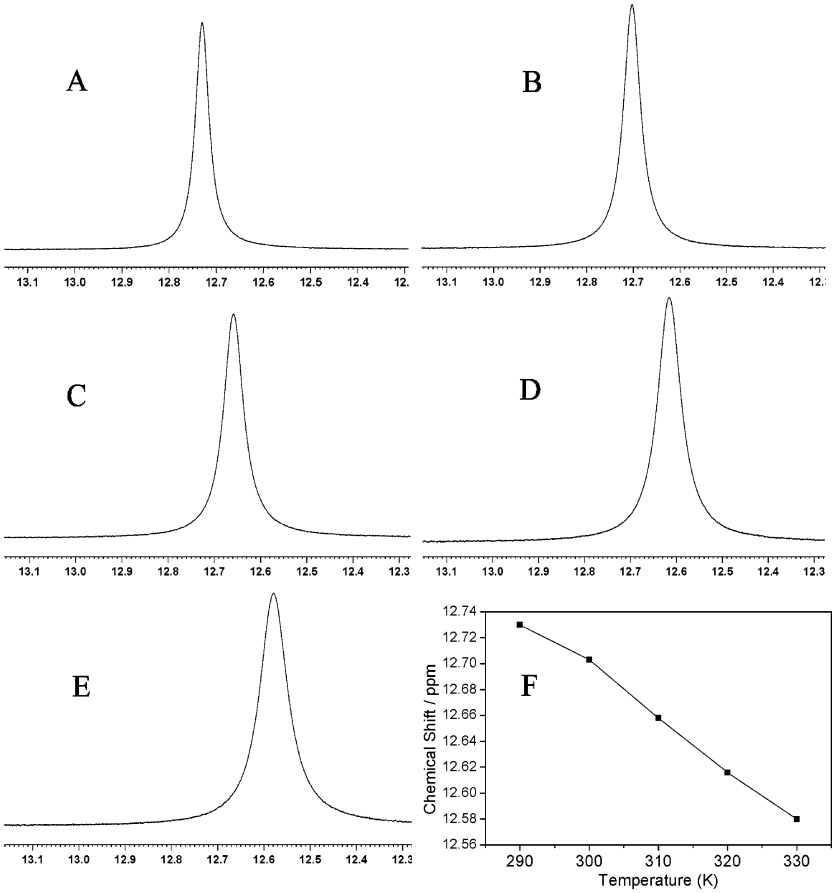

Figure 4. Temperature-dependent ^{1}H NMR spectra for TPI submicrotubes at (A) 290 K, (B) 300 K, (C) 310 K, (D) 320 K, and (E) 330 K were selected to determine the temperature coefficient of the ^{1}H NMR chemical shift of the active H atom connected to N atom. The results are 12.73, 12.70, 12.66, 12.62, and 12.58 ppm respectively. (F) The chemical shift-temperature curve.

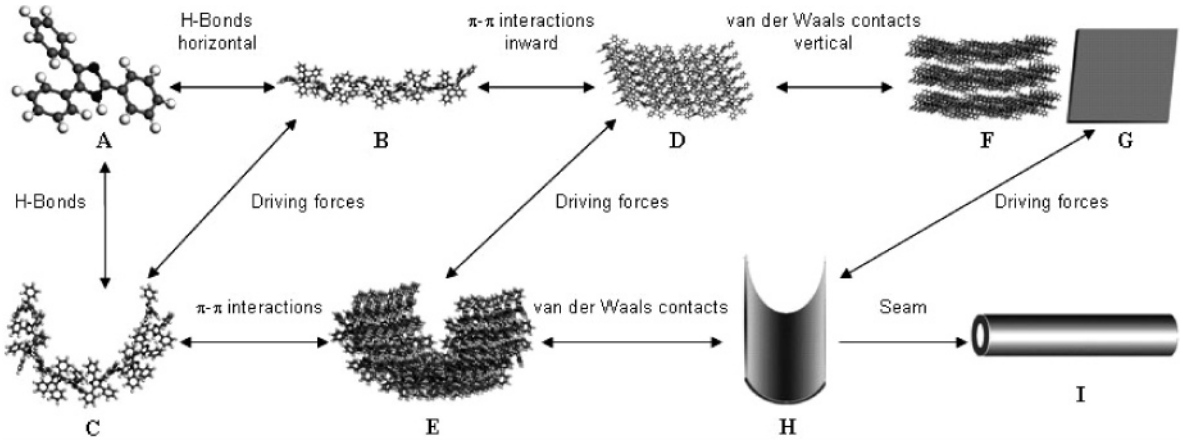

Figure 5. Schematic representation for the formation of TPI submicrotube. (A) Optimized geometry of single TPI molecule. (B and C) Linear and curled motifs of TPI supramolecular H-bonded chains. (D and E) Flat and curled monolayer sheets from the two motifs of chains. (F) Multilayer sheet by stacking of the monolayers. (G−I) Sketch maps of the multilayer flat lamellar, curled lamellar, and tubular structures, respectively. The driving forces are described in the text.

peak arising from phenyl rings in the tube samples shows obvious red shift as compared with that of the monomer, which can also be attributed to the strong $\pi-\pi$ interactions in the nanotubes that make the TPI molecules more planar and therefore make the π bonds more delocalized.

In principle, two typical optimized supramolecular chains, linear (Figure 5B) and curled (Figure 5C), can be expected depending on the zigzag and revolving motifs of the intermolecular H-bonds. Correspondingly, flat (Figure 5D) and curled (Figure 5E) monolayer sheet-like structures can be constructed respectively via the $\pi-\pi$ interactions between the chains. The monolayer sheets can stack into flat (Figure 5F and G) and curled (Figure 5H) multilayer lamellar structures, respectively, with certain thickness via interlayer van der Waals contacts. The formation of the multilayered lamellar structures is due to the efficient cooperation of three chemically orthoganol and spatially independent noncovalent interactions as shown in Figure 5. Theoretical calculations indicate that the energy of the linear chain is 40 kJ mol^{-1} lower than that of the curled one if there was no other influence from surroundings. In our system, however, the energy of the two chains should be much closer since on

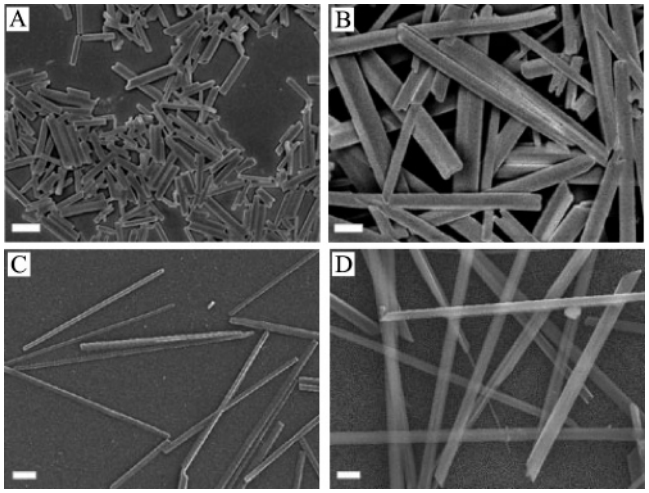

Figure 6. SEM images of TPI submicrotubes obtained under different experimental conditions. (A) at 25 °C, scale bar is 500 nm. (B) at 70 °C, scale bar is 500 nm. (C and D) at 80 °C, scale bars are 1 μm. 20 s sonication treatment was adopted in (A−C), while no ultrasonic treatment was employed in (D).

one hand the flat sheets have a tendency to roll in order to reduce the surface energy in water and on the other hand the nonplanar character of TPI molecule makes the flat sheets asymmetric both in substituents and in charge distribution at the two sides, which is profitable for the rolling of the flat sheets in that it induces the asymmetric acting forces on the two sides, just like the bend of bimetallic strips.[32] The rolling of the flat sheets into the curled ones is favorable since this can reduce both the surface energy and the tension brought by the asymmetry of the sheets. Finally, the curled sheets will seam into tubes (Figure 5I) by the ring-closure of the curled chains through the formation of new H-bonds between the TPI molecules at the two edges. About 30 kJ mol^{-1} more energy will be further released in the formation of new H-bonds during the ring-closure process, which makes the tubular structure to be the most thermodynamically stable one.

According to the formation mechanism proposed in Figure 5, the size of the as-prepared TPI submicrotubes should be controllable by varying the energy supply into the system by means of changing the temperature of the poor solvent and/or the sonication time. This was testified by the results of a series of contrast experiments. First, both the length and the diameter increase obviously with the rise of the temperature of the water into which the stock solution was injected although the influence on length is more significant. For example, with the sonication time fixed at 20 s, when the temperatures are 25, 70, and 80 °C, the lengths of the tubes are 1, 5, and 10 μm, respectively, and the diameters are 150, 300, and 500 nm, respectively (Figure 6A−C). The changing of the sizes here must be related to the character of the poor solvent since all the other factors remain the same. The solubility of TPI in water is dependent strongly on temperature. When 400 μL of TPI stock solution (10^{-3} M) was injected into 10 mL of water with temperature higher than 85 °C, only monomer disperse system can be obtained, which is proved by the absorption spectra and the clarity of the system. According to the above discussions, it is reasonable that the last process shown in Figure 5 (seam through ring-closure) is almost irreversible because the tubular structure is more stable than other structures, whereas most of the other processes should be reversible in that the energies of the two motifs are close to each other. When the stock solutions were injected into cooler water, the TPI molecules nucleate, aggregate, and close the H-bond rings rapidly to form tubes with small sizes. While when the stock solutions were injected into water with higher temperatures, for example, 80 °C, the initial nuclei induced by the changing of the solvent surroundings are much fewer because a portion of TPI molecules are dissolved. Moreover, the seam of the curled sheets is slowed significantly because the formation of H-bonds is more difficulty at higher temperature.[33] Therefore, there are enough time and TPI sources for the lamellar structures to grow in both dimensions before the seam process; as a result, TPI tubes with larger length and diameter can be prepared.

Second, the sonication treatment plays another role in controlling the tube sizes. That is to say, when the temperature of the poor solvent is lower than 50 °C, the sonication time can hardly affect the tube size, while when the temperature is higher, both the length and the diameter decrease with the prolonging of sonication time although the diameter changes to a much more degree. For example, when 0 and 20 s ultrasonic treatments were carried out at 80 °C, tubes with diameters of 1 μm and 300 nm were obtained, respectively, whereas the lengths are 8 and 6 μm, respectively (Figure 6C and D). There are essential differences between the manners through which calefaction and sonication supply energy to the system. For example, calefaction supplies continuous energy through heat conduction while sonication supplies much less energy than calefaction through radiation. Moreover, sonication can hardly influence the solubility of TPI. Actually the main role of sonication here is the high frequency vibration for dispersing the stock solution into the poor solvent quickly and uniformly and then accelerating the aggregation of TPI molecules in the poor solvent by increasing the collision probability. When the solution was injected into cooler water, the aggregation and ring-closure are rapid no matter there is sonication or not so that the size can hardly be influenced. In water with higher temperature, however, the sonication can accelerate the aggregation and the ring-closure of the TPI molecules; therefore, there is not enough time for the sheet-like structures to grow in both the length and width dimensions, resulting in the decrease of both the diameter and the length.

The as-fabricated TPI submicrotubes show interesting size-dependent optical property (Figure 7). When the diameter of the tubes increased from 120 to 500 nm, the $S_0 \rightarrow S_1$ band exhibits a red shift and simultaneously a new band in the region of 330−350 nm emerges and gradually becomes predominant, which also shifts to lower energy side at the expense of the $S_0 \rightarrow S_1$ transition. This can be attributed to the factor that as the diameter decreases, the increase of the

(32) Saupe, G. B.; Waraksa, C. C.; Kim, H. N.; Han, Y. J.; Kaschak, D. M.; Skinner, D. M.; Mallouk, T. E. *Chem. Mater.* **2000**, *12*, 1556.

(33) Wallen, S. L.; Palmer, B. J.; Garrett, B. C.; Yonker, C. R. *J. Phys. Chem.* **1996**, *100*, 3959.

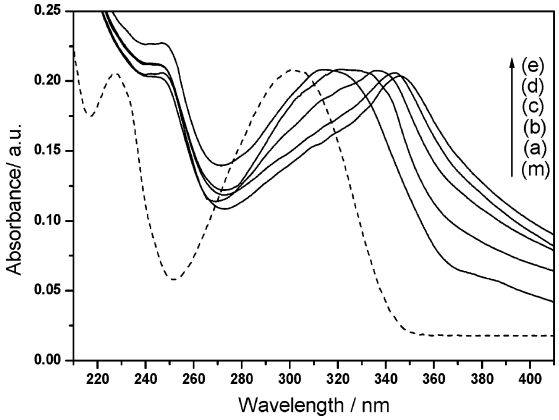

Figure 7. UV−visible absorption spectra of TPI submicrotubes dispersed in water with different diameters: (a) 120, (b) 180, (c) 250, (d) 300, and (e) 500 nm. For comparison, the spectrum of TPI monomers (m) is also displayed.

surface area causes lattice softening, and therefore the Coulombic interaction energies between molecules become smaller, resulting in the wider band gaps.[9]

The TPI submicrotubes present strong luminescence with a fluorescence quantum yield over 50%, comparable with those of some widely used inorganic light-emitting nanomaterials.[34] The tubes dispersed in water can retain their shape and size without obvious aggregation for at least 6 months, and powdered tubes separated from water can sustain the temperature as high as 160 °C for several hours under the protection of nitrogen. In view of their single crystalline structure, intense luminescence, size-dependent optical properties, and good stability, the submicrotubes are expected to have potential applications in the design of novel optical and optoelectronic devices.

(34) Ebenstein, Y.; Mokari, T.; Banin, U. *Appl. Phys. Lett.* **2002**, *80*, 4033.

Conclusion

In summary, the single crystalline submicrotubes from a small organic molecule, 2,4,5-triphenylimidazole, were prepared with a facile method. The as-fabricated tubes were proved to be obtained from the rolling and seaming of a 2D lamellar structure constructed via the cooperation of three chemically orthoganol and spatially independent noncovalent interactions; namely, H-bond, $\pi-\pi$ interaction, and van der Waals contact. The tubes show interesting size-dependent optical properties, intense luminescence, and good stability, which may allow them to find their potential applications in optoelectronic devices. This work may provide a brand-new alternative approach to the design and fabrication of tubular structures from small organic molecules with tunable sizes.

Acknowledgment. This work was supported by National Natural Science Foundation of China (Grants 50221201, 90301010, and 20373077), the Chinese Academy of Sciences, and the National Research Fund for Fundamental Key Project 973. We thank Professor Shouke Yan and Professor Xiaolong Chen for their helpful discussions.

Supporting Information Available: The comparison between the UV−visible absorption spectra of TPI monomers and TPI tubes with a diameter of 250 nm; the assignation of the absorption band of TPI monomer and TPI tubes. This material is available free of charge via the Internet at http://pubs.acs.org.

CM051949T